FEBS Letters 491 (2001) 26–29 FEBS 24556

Structure of the ExoS GTPase activating domain

Martin Würtele[a], Louis Renault[a], Joseph T. Barbieri[b], Alfred Wittinghofer[a], Eva Wolf[a,*]

[a] *Max-Planck-Institut für molekulare Physiologie, Abteilung Strukturelle Biologie, Otto-Hahn-Str. 11, 44227 Dortmund, Germany*
[b] *Microbiology and Molecular Genetics, Medical College of Wisconsin, Milwaukee, WI 53226, USA*

Received 8 December 2000; accepted 8 January 2001

First published online 29 January 2001

Edited by Hans Eklund

Abstract ***Pseudomonas aeruginosa*** **is an opportunistic bacterial pathogen of great medical relevance. One of its major toxins, exoenzyme S (ExoS), is a dual function protein with a C-terminal Ras-ADP-ribosylation domain and an N-terminal GTPase activating protein (GAP) domain specific for Rho-family proteins. We report here the three-dimensional structure of the N-terminal domain of ExoS determined by X-ray crystallography to 2.4 Å resolution. Its fold is all helical with a four helix bundle core capped by additional irregular helices. Loops that are known to interact with Rho-family proteins show very large mobility. Considering the importance of ExoS in** ***Pseudomonas*** **pathogenicity, this structure could be of interest for drug targeting.**

Key words: Toxin; ExoS; GTPase activating protein; X-ray structure; *Pseudomonas aeruginosa*

1. Introduction

Pseudomonas aeruginosa is a major opportunistic human pathogen. In part due to its natural resistance against antibiotics and disinfectants, it is a significant source of bacterial infections in hospitalised patients, like for example severe burn victims. Furthermore, long term colonisation of the lungs by *P. aeruginosa* is the leading cause of mortality of cystic fibrosis patients [1].

Exoenzyme S (ExoS) is essential for virulence as the disruption of its gene drastically decreases the lethality of *P. aeruginosa* [2]. It is secreted into host cells by a type III secretion mechanism. Whereas the C-terminal domain of ExoS (residues 234–453) shows Ras-ADP-ribosylation activity [3], a Rho-specific GTPase activating protein (GAP) activity has been localised in its N-terminal domain (residues 1–234) [4]. The Rho family proteins Rho, Rac and Cdc42 are GTP binding proteins acting like molecular switches that are involved in the regulation of actin cytoskeleton rearrangements in a large array of signaling processes [5]. Because Rho-family GTP binding proteins also regulate macrophage-mediated phagocytosis, it is thought that the N-terminal Rho-family-GAP activity of ExoS is essential for protection of *P. aeruginosa* from attack by the host immune system [4]. A similar function of macrophage phagocytosis protection has been reported for the ExoS-GAP homologue YopE of *Yersinia* sp. [6,7]. Whereas ExoS in *Pseudomonas* and YopE in *Yersinia* are thus thought to be part of a protective mechanism of bacteria against host phagocytic cells, the ExoS homologue SptP in *Salmonella* seems to have a somewhat different function. In this organism, the GAP activity of SptP is part of an intricate mechanism responsible for transforming non-phagocytic cells temporarily so that they can internalise the bacterium. GAP activity of SptP would in this model restore normal cytoskeleton function after injection of the guanine-nucleotide exchange factor (GEF) SopE induces endocytosis of the bacteria through Rho-family-mediated cytoskeletal rearrangements [8,9].

We have recently solved the crystal structure of the complex between the ExoS GAP domain (termed ExoS-N from now on) and human Rac1 [10]. Because of the potential importance of ExoS-N as a drug target, because the actual target of drugs would be ExoS-N alone rather than the complex, and in order to better understand structural determinants of the domain during the enzymatic reaction, we have also solved the structure of uncomplexed ExoS-N.

2. Materials and methods

Selenomethionine-substituted ExoS (96–234) was expressed as a recombinant GST fusion protein with the additional N-terminal amino acids Gly–Ser–Ala (after thrombin cleavage) and a C-terminal haemagglutinin-tag using the Met auxotroph *Escherichia coli* strain B834 grown on minimal medium supplemented with SeMet. After affinity purification of the protein and concentration to 20 mg/ml in 25 mM Tris-buffer pH 7.5, ExoS-N crystals were grown and improved by microseeding at 20°C in a solution containing 16% PEG 6000, 0.2 M $(NH_4)_2SO_4$, 10 mM $MgCl_2$ and 100 mM Na–cacodylate pH 5.5 using the hanging drop method. They were frozen in liquid N_2 using precipitant solution supplemented to 30% PEG 6000, 2% isopropanol and 4% ethylene glycol. Two different crystal forms were obtained under these conditions: triangular plates, which belonged to space group P1 and did not diffract very well and a rectangular crystal, which belonged to the orthorhombic space group $C222_1$ and diffracted to 2.1 Å resolution. Unit cell dimensions of the orthorhombic crystal were $a = 42.9$ Å, $b = 55.7$ Å and $c = 107.5$ Å with one ExoS-N molecule per asymmetric unit.

A 2.4 Å in house data set of this crystal was collected using a Nonius rotating Cu-anode ($\lambda_0 = 1.54$ Å) with a MAR imaging plate detector (MAR345). Additionally, multiwavelength anomalous dispersion (MAD) data were collected at three wavelengths corresponding to the peak ($\lambda_1 = 0.9790$ Å), inflection point ($\lambda_2 = 0.9789$ Å) and a high energy remote point above the Se absorption edge ($\lambda_3 = 0.8856$ Å) using the BM-14 beamline at ESRF, Grenoble, France.

Reflections were integrated with DENZO and scaled with SCALEPACK [11]. Two of the three Se atoms of ExoS-N could be identified using Patterson analysis. The third Se atom was localised in a region

*Corresponding author. Fax: (49)-231-133 2699.
E-mail: eva.wolf@mpi-dortmund.mpg.de

Abbreviations: ExoS, exoenzyme S; GAP, GTPase activating protein; MAD, multiwavelength anomalous dispersion; GEF, guanine-nucleotide exchange factor; r.m.s., root mean square

PII: S0014-5793(01)02105-6

with high B-factors and its refinement lead to a low occupancy. SHARP [12] was used to estimate experimental phases at 2.1 Å, giving final figures of merit of 0.65 and 0.71 for centric and acentric reflections, respectively. After density modification using DM [13], the resulting maps allowed identification of most of the ExoS-N chain. Chain building and examination was carried out with Xfit [14]. The obtained model was refined using CNS [15] with the 2.4 Å home-collected data set, because it led to the lowest crystallographic R-factor. Refinement against the MAD data sets resulted in higher R-factors, which could be due to radiation damage of the crystal. For best results, experimental phases were included in the refinement using maximum likelihood with incorporated experimentally determined phase probability in terms of the Hendrickson and Lattman coefficients (MLHL target of CNS)[16]. The final model consists of amino acids 102–234 of ExoS-N as well as the first residue of the haemagglutinin-tag and 65 water molecules. It was refined to an overall crystallographic R-factor of 25.7% and R-free of 26.7%. PROCHECK [17] revealed no amino acids with unfavourable Φ,Ψ main chain angles.

Coordinates and structure factors have been deposited in the protein data bank (pdb) under accession number 1he9.pdb.

3. Results and discussion

The structure of ExoS-N was solved by SeMet-MAD phasing using the crystal belonging to the orthorhombic space group $C222_1$. Fig. 1 shows details of the experimental electron density map, which allowed the identification and building of most of the ExoS-N protein chain. Amino acids 135–143 and 186–189 refined to very high B-factors and could not be identified with the same clarity as the amino acids shown in Fig. 1. The final model includes residues 102–234 of ExoS and 65 water molecules and is characterised by a final R-factor of 25.7% (R-free = 26.7%). The final crystallographic R-factor could not be improved by further refinement, perhaps due to the relatively large flexibility of the protein as indicated by the overall B-factor of 62.3 Å^2 (Table 1).

ExoS-N consists of a single almost all-helical protein domain of about 130 amino acids. Its overall structure is shown in Fig. 2. The core of the domain is formed by a four helix bundle built up by parts of the kinked helix 1, helix 3, helix 4 and the long C-terminal helix 7. One side of this structure is capped by three additional helices (H2, H5 and H6), as well as a very small two stranded β-sheet (S1, S2). Between the second and the third helix, as well as between the fifth and the sixth helix, two prominent loops protrude sideways. These two bulges contain the most conserved sequences in the GAP domain of ExoS and the related toxins ExoT, SptP of *Salmonella typhimurium* and YopE of *Yersinia* sp. As shown in our previous structure, they are important Rac binding regions, bulge I being involved in the stabilisation of the catalytic Gln61 of Rac and bulge II stabilising the catalytic Arg 146 of ExoS and making direct interactions with the oxygens of the ribose of GDP [10].

Compared with our previously reported structure of the ExoS-N–Rac complex[10], the first six amino acids of helix 1 (residues 96–101) of ExoS-N can not be identified in the electron density maps. This indicates that in the complex they are probably stabilised by the interaction of this helix with Rac. Again compared to the complex, five additional C-terminal amino acids could be seen in the electron density maps, indicating that helix 7 is in fact larger than observed in the complex structure. The ExoS-N structure therefore confirms by MAD phasing the unique ExoS-N fold that we have recently determined in the context of the ExoS-N–human Rac1 complex structure (Fig. 3). The overall root mean square (r.m.s.) deviation for corresponding Cα atoms of complexed and unbound ExoS-N is 0.83 Å. The highest deviation between both models is localised on the regions surrounding the two important bulges (r.m.s. deviations of about 1.2 Å), whereas the four helix bundle region shows very small devia-

Table 1
X-ray data collection and refinement statistics

	λ_0	λ_1	λ_2	λ_3
Data collection				
Wavelength (Å)	1.54	0.9789	0.9790	0.8856
Resolution range (Å)[a]	20–2.4 (2.49–2.4)	30–2.1 (2.15–2.1)	30–2.1 (2.18–2.1)	30–2.1 (2.18–2.1)
Number of reflections	68947	143634	116369	112509
Number of unique reflections	5272	14016	13791	13429
Completeness (%)[a]	95.3 (98.4)	98.1 (90.4)	96.5 (82.2)	94 (88.6)
I/σ[a]	34 (8)	24.3 (2.9)	27.1 (2.6)	23 (3.2)
R-sym (%)[a]	5.3 (17.5)	3.4 (25.8)	3.2 (30)	3.6 (28.9)
Phasing Power (Ano/Iso)	–	3.5/8.3	2.8/6.8	2.5/–
Refinement				
Resolution range (Å)	20–2.4			
Reflections	5237			
Atoms	1067			
R-cryst (%)	25.7			
R-free (%)[b]	26.7			
Average B-factor:				
Protein (Å^2)	62.4			
Solvent (Å^2)	61.6			
r.m.s.d. from ideal values:				
Bond lengths (Å)	0.016			
Bond angles (°)	2.06			
Ramachandran plot[c]:				
Residues in most favoured regions	89.7			
Residues in additionally allowed regions		10.3		

[a]Values in parentheses correspond to highest resolution shell.
[b]The R-free factor was calculated with 10% of the data omitted from structure refinement.
[c]Data calculated using the program PROCHECK [17].

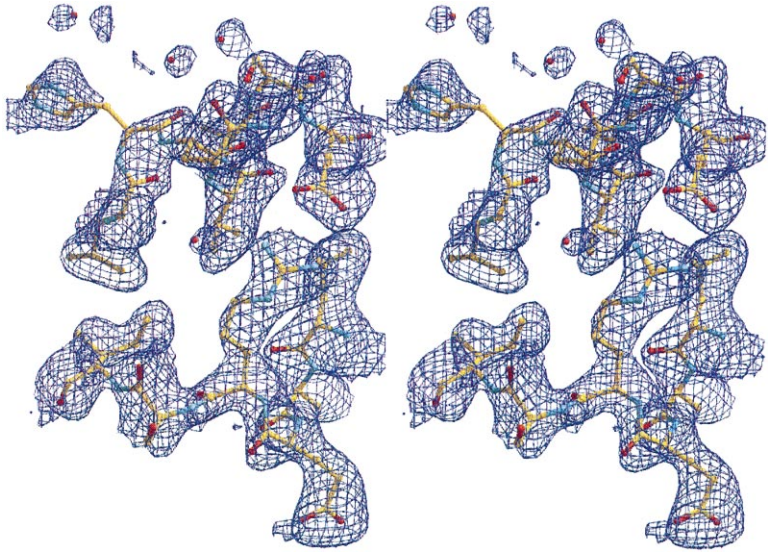

Fig. 1. Stereo view of the experimental electron density map of the four helix bundle region of ExoS-N contoured at 1 σ. Upper part shows the C-terminal helix H7 with Glu216, which forms a salt bridge to Arg174 of helix H4 (lower part). This figure was produced with Xfit [14].

tions (r.m.s. deviations of 0.6 Å). Interestingly and contrary to the situation in the ExoS-N–Rac complex, the bulge regions have the highest B-factors of the structure, as indicated in Fig. 4. This finding suggests that they are ordered during substrate binding, thus following an induced fit mechanism.

The functional importance of flexible regions in substrate binding has been described for a series of proteins and especially enzymes [18]. In the case of ExoS, one important role of the flexibility of the bulge regions could be to allow for an adjustment of the ExoS structure to different host cell target proteins like Rho, Rac and Cdc42. Section 2 data [4] as well as our previous structure [10] indeed support the conclusion that ExoS binds with similar affinity to all three GTPases. We can however not entirely rule out that the conformational changes and the increased mobility of the bulge regions observed in the structure of uncomplexed ExoS are at least partly influenced by crystal packing and the absence of truncated parts of the molecule. In the case of the first region with high B-factors (bulge I) there are no prominent crystal contacts that could influence its conformation. In the case of bulge II however, at least part of the observed r.m.s. deviation could be explained by crystallographic clashes that would result if the chain had the same conformation as in the complex structure.

The position of the side-chain of the catalytic arginine Arg146 of ExoS-N can be located in both the experimental electron density and omit maps of the final model. This density indicates that Arg146 occupies a slightly different conformation in the uncomplexed protein structure as compared to the complex structure. In this conformation, the arginine is not stabilised by the bulge II residues Gly185 and Thr186 as it is in the complex structure. This could indicate that the in-

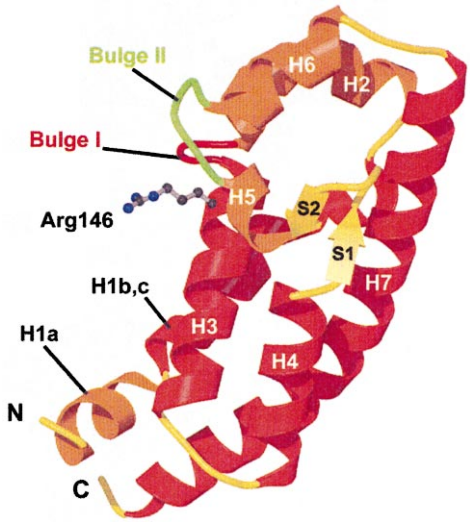

Fig. 2. The ExoS-N fold. Helices that form the four helix bundle core motif (H1bc, H3, H4, H7) are drawn in darker red, other helices (H1a, H2, H5, H6) in orange. Bulge I and Bulge II are highlighted in red and green, respectively. The catalytic arginine (Arg146) is drawn as a ball-and-stick model. This figure was drawn with Molscript [32].

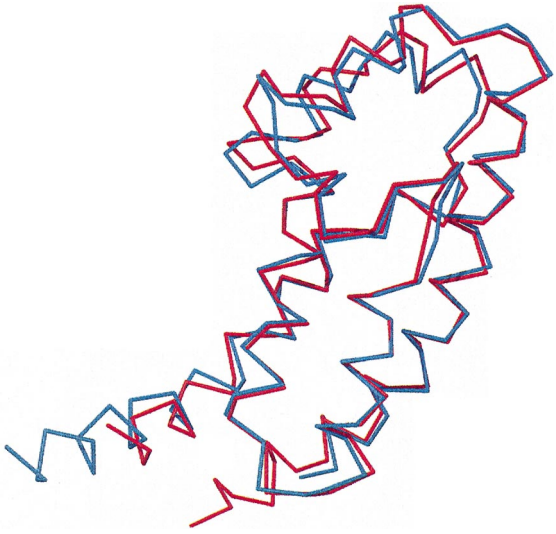

Fig. 3. Superposition of Cα traces of ExoS-N structures. The Cα trace of the structure of uncomplexed ExoS-N (red) is superimposed on to the ExoS-N structure from the ExoS-N–Rac1 complex (blue) [10].

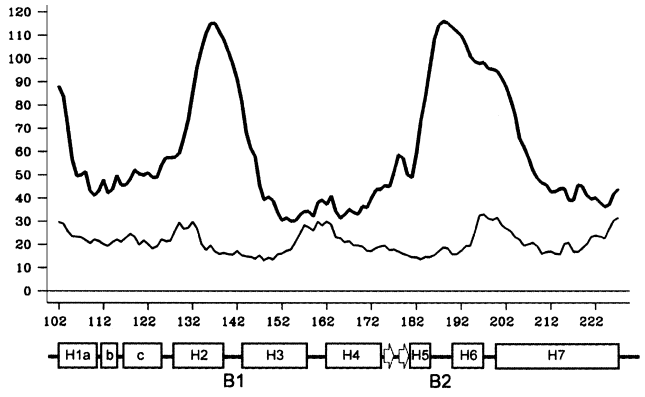

Fig. 4. B-factor plot of ExoS-N. Average B-factors (in Å^2) along ExoS-N chain were calculated and plotted using the program bplot [13]. The two regions with high B-factors correspond to the bulge I and bulge II regions, respectively. Upper curve: uncomplexed ExoS-N, lower curve: ExoS-N–Rac complex. Secondary structure is plotted beneath the graph. B1, bulge I; B2, bulge II.

creased motility of the bulges surrounding the catalytic arginine has the function of increasing the degrees of freedom of the catalytic arginine for better GTPase interaction.

The structure of isolated or GTPase-bound eukaryotic GAPs for Ras [19–21], Rho [22–24], Rab [25], Ran [26] and Arf [27] proteins have been solved. Ran GAPs and Arf GAPs have an α,β-fold, the others are all-helical proteins. A common ancestry has been proposed for Ras and RhoGAPs based on structural similarities [28–31]. As outlined in our earlier report, ExoS-N has no structural homology to any of these proteins. It has probably acquired an enzymatic mechanism very similar to eukaryotic GAPs by convergent evolution. An important feature that outlines this, is the different arrangement of the four helix bundles towards the GTPase, the different contacting amino acids, as well as the presence of the catalytic arginine on a helix rather than a surface loop. In contrast to ExoS, no dramatic changes in the mobility (B-factors) of interacting residues can be detected if the complexed and unbound structures of RasGAP [19,20] or RhoGAP [22,23] are compared. The structure of the unbound GAP-related domain from neurofibromin, however, could represent a situation similar to ExoS, since it has a similarly high overall B-factor and elevated B-factors in the GTPase contacting finger-loop [21].

To conclude, the structure reported here confirms the uniqueness of the ExoS-N fold as compared to eukaryotic GAPs by an independent phasing method. The structure of the ExoS-N monomer resembles globally the structure of ExoS-N in complex with Rac, shows however increased mobility and conformational changes of the important bulge I and bulge II Rac1 interacting regions.

Acknowledgements: We thank Sean McSweeny, Elspeth Gordon and ESRF for beam-time allocation and help during data collection. J.T.B. was supported by NIH AI30162.

References

[1] Stover, C.K. et al. (2000) Nature 406, 959–964.
[2] Coburn, J. (1992) Curr. Top. Microbiol. Immunol. 175, 133–143.
[3] Ganesan, A.K., Frank, D.W., Misra, R.P., Schmidt, G. and Barbieri, J.T. (1998) J. Biol. Chem. 273, 7332–7337.
[4] Goehring, U.M., Schmidt, G., Pederson, K.J., Aktories, K. and Barbieri, J.T. (1999) J. Biol. Chem. 274, 36369–36372.
[5] Bishop, A.L. and Hall, A. (2000) Biochem. J. 348, 241–255.
[6] Pawel-Rammingen, U. et al. (2000) Mol. Microbiol. 36, 737–748.
[7] Black, D.S. and Bliska, J.B. (2000) Mol. Microbiol. 37, 515–527.
[8] Fu, Y.X. and Galán, J.E. (1999) Nature 401, 293–297.
[9] Hardt, W.D., Chen, L.M., Schuebel, K.E., Bustelo, X.R. and Galán, J.E. (1998) Cell 93, 815–826.
[10] Würtele, M., Wolf, E., Pederson, K.J., Buchwald, G., Ahmadian, M.R., Barbieri, J.T. and Wittinghofer, A. (2000) Nature Struct. Biol. 8, 23–26.
[11] Otwinowski, Z. and Minor, D.L. (1997) Methods Enzymol. 276, 307–326.
[12] de La Fortelle, E. and Bricogne, G. (1997) Methods Enzymol. 276, 472–494.
[13] CCP4, (1991) Acta Crystallogr. D Biol. Crystallogr. 50, 275–278.
[14] McRee, D.E. (1999) J. Struct. Biol. 125, 156–165.
[15] Brünger, A.T. et al. (1998) Acta Crystallogr. D Biol. Crystallogr. 54, 905–921.
[16] Pannu, N.S., Murshudov, G.N., Dodson, E.J. and Read, R.J. (1998) Acta Crystallogr. D Biol. Crystallogr. 54, 1285–1294.
[17] Laskowski, R.A. and MacArthur (1993) J. Appl. Crystallogr. 26, 283–291.
[18] Yon, J.M., Perahia, D. and Ghélis, C. (1998) Biochimie 80, 33–42.
[19] Scheffzek, K., Lautwein, A., Kabsch, W., Ahmadian, M.R. and Wittinghofer, A. (1996) Nature 384, 591–596.
[20] Scheffzek, K. et al. (1997) Science 277, 333–338.
[21] Scheffzek, K., Ahmadian, M.R., Wiesmüller, L., Kabsch, W., Stege, P., Schmitz, F. and Wittinghofer, A. (1998) EMBO J. 15, 4313–4327.
[22] Barett, T. et al. (1997) Nature 385, 458–461.
[23] Rittinger, K., Walker, P.A., Eccleston, J.F., Smerdon, S.J. and Gamblin, S.J. (1997) Nature 389, 758–762.
[24] Nassar, N., Hoffman, G.R., Manor, D., Clardy, J.C. and Cerione, R.A. (1998) Nature Struct. Biol. 5, 1047–1052.
[25] Rak, A. et al. (2000) EMBO J. 19, 5105–5113.
[26] Hillig, R.C. et al. (1999) Mol. Cell 3, 781–791.
[27] Goldberg, J. (1999) Cell 96, 893–902.
[28] Bax, B. (1998) Nature 392, 447–448.
[29] Rittinger, K., Taylor, W.R., Smerdon, S.J. and Gamblin, S.J. (1998) Nature 392, 448–449.
[30] Souchet, M., Poupon, A., Callebaut, I., Léger, I., Mornon, J.P., Bril, A. and Calmels, T.P.G. (2000) FEBS Lett. 477, 99–105.
[31] Scheffzek, K., Ahmadian, M.R. and Wittinghofer, A. (1998) Trends Biochem. Sci. 23, 257–262.
[32] Kraulis, P.J. (1991) J. Appl. Crystallogr. 24, 946–950.